Research article

Disruption of spinal cord white matter and sciatic nerve geometry inhibits axonal growth *in vitro* in the absence of glial scarring

David B Pettigrew[2], Kristina P Shockley[1] and Keith A Crutcher*[1]

Address: [1]Department of Neurosurgery, University of Cincinnati College of Medicine, Cincinnati, Ohio 45267-0515, U.S.A and [2] Dept. of Neurobiology and Anatomy University of Texas-Houston Health Science Center P.O. Box 20708 Houston, Texas, U.S.A

E-mail: David B Pettigrew - David.Pettigrew@uth.tmc.edu; Kristina P Shockley - shockley23@hotmail.com; Keith A Crutcher* - crutchka@email.uc.edu

*Corresponding author

Published: 31 May 2001

BMC Neuroscience 2001, **2**:8

Received: 13 March 2001
Accepted: 31 May 2001

This article is available from: http://www.biomedcentral.com/1471-2202/2/8

Abstract

Background: Axons within the mature mammalian central nervous system fail to regenerate following injury, usually resulting in long-lasting motor and sensory deficits. Studies involving transplantation of adult neurons into white matter implicate glial scar-associated factors in regeneration failure. However, these studies cannot distinguish between the effects of these factors and disruption of the spatial organization of cells and molecular factors (disrupted geometry). Since white matter can support or inhibit neurite growth depending on the geometry of the fiber tract, the present study sought to determine whether disrupted geometry is sufficient to inhibit neurite growth.

Results: Embryonic chick sympathetic neurons were cultured on unfixed longitudinal cryostat sections of mature rat spinal cord or sciatic nerve that had been crushed with forceps *ex vivo* then immediately frozen to prevent glial scarring. Neurite growth on uncrushed portions of spinal cord white matter or sciatic nerve was extensive and highly parallel with the longitudinal axis of the fiber tract but did not extend onto crushed portions. Moreover, neurite growth from neurons attached directly to crushed white matter or nerve tissue was shorter and less parallel compared with neurite growth on uncrushed tissue. In contrast, neurite growth appeared to be unaffected by crushed spinal cord gray matter.

Conclusions: These observations suggest that glial scar-associated factors are not necessary to block axonal growth at sites of injury. Disruption of fiber tract geometry, perhaps involving myelin-associated neurite-growth inhibitors, may be sufficient to pose a barrier to regenerating axons in spinal cord white matter and peripheral nerves.

Background

Axonal regeneration is limited in the central nervous system (CNS) following injury [1]. This regeneration failure appears not to be due to intrinsic limitations of mature neurons to grow axons but, rather, to nonpermissive properties of the CNS environment [2]. One theory is that white matter contains putative inhibitors of axonal growth associated with myelin [3-16]. However, extensive axonal growth occurs *in vivo* from neurons transplanted into white matter, providing that disruption of tissue organization and glial scarring are minimized [17,18]. In contrast, when tissue disruption was signifi-

cant and accompanied by glial scarring, including astrogliosis and the upregulation of chondroitin sulfate proteoglycans (CSPGs), axonal growth stopped in areas of CSPG expression. These studies have questioned the role of myelin-associated inhibitors in preventing axonal regeneration and, together with *in vitro* studies showing inhibition of neurite growth by CSPGs [19,20,21], implicate the expression of CSPGs at injury sites in causing regeneration failure.

However, these transplantation studies involved survival periods of over two days so that the contributions of glial scarring and disruption of the organization of cells and molecules that were present prior to injury (disrupted geometry) cannot be evaluated separately. This limitation can be overcome by culturing neurons on cryostat sections where both the success and orientation of neurite growth on white matter have been shown to depend on the geometry of the underlying fiber tract [22]. Neurites on white matter are restricted to a parallel orientation, consistent with successful axonal growth *in vivo* from neuronal transplants [17,18,23-28]. Given the dependence of neurite growth on tissue geometry, we sought to determine whether disruption of this geometry is sufficient to inhibit neurite growth in the absence of glial scarring.

Adult rat spinal cord or sciatic nerve was crushed with forceps *ex vivo* and immediately frozen to prevent additional changes within the tissue, such as glial scarring, Wallerian degeneration and formation of bands of Büngner. Neurite growth on the uncrushed portions of spinal cord white matter or nerve was extensive and mostly parallel to the tract but significantly inhibited by crushed white matter or nerve. In contrast, neurites were unimpeded by crushed gray matter. These data suggest that disruption of CNS white matter and peripheral nerve geometry is sufficient to prevent axonal regeneration. The disrupted tissue elements involved in white matter may be oligodendrocytes and/or myelin since neurites were not inhibited by crushed gray matter. Therefore, regeneration failure in CNS white matter may be partly due to the persistence of disrupted myelin. In peripheral nerves, acute injury may also prevent regeneration but successful regeneration may occur following chronic changes involving clearance of putative inhibitors.

Results

Histology of crushed tissue

Crushed portions of spinal cord white matter (Fig. 1A) and sciatic nerves (Fig. 1D) were characterized by increased optical density compared with uncrushed tissue when viewed with phase-contrast optics. This is similar to the appearance of fiber tracts sectioned transversely [22]. No increase in optical density was evident within crushed gray matter (Fig. 1A). GFAP (Fig. 1B) and myelin (Fig. 1C), which are normally aligned mostly in parallel with the fiber tracts, appeared to be disrupted within crushed white matter. Patches of increased GFAP immunoreactivity could occasionally be seen within crushed tissue (Fig. 1B) but not to the extent or morphology normally seen in glial scars [19,29]. Moreover, no increase in CSPG immunoreactivity was present within crushed white matter (data not shown). A line of complete tissue disruption could often be seen midway through crushed segments of spinal cord white matter (Fig. 1A,B,C).

Neurite growth on sections of crushed spinal cord

The distribution of neurons was heterogeneous on uncrushed spinal cord white matter but the behavior of neurites was independent of cell density. Therefore, for purposes of demonstration, the photomicrographs shown are generally of cases from higher density cultures. Neurite growth on uncrushed spinal cord white matter was extensive and mostly constrained to an orientation parallel to the longitudinal axis of the tract (Fig. 2A,C). These neurites, however, were generally inhibited from extending onto crushed white matter. In some cases, neurites terminated abruptly at the border of crushed white matter (Fig. 2A,C). In other cases, the neurites became increasingly disoriented as they approached the border of the crush and were closely associated with other neurites, appearing to use each other as a substrate (Fig. 2E), similar to neurites that occasionally extend over cross-sections of white matter [22]. Neurites that extended from neurons attached directly to crushed white matter often grew in non-parallel orientations and frequently appeared to use each other as a substrate (Fig. 2C). In other cases, neurons on crush sites showed minimal neurite outgrowth (Fig. 2E). Interestingly, neurites were generally unaffected by crushed gray matter (Fig. 2E, G).

The numbers of neurons that attached to CNS white matter were limited and large segments of uncrushed white matter often contained no neurons at all, even with the improved culture conditions utilizing Neurobasal medium. Furthermore, while neurites generally appeared to be inhibited by crushed white matter, this inhibition was not absolute as neurites occasionally crossed onto crushed tissue. To determine more precisely if crushed white matter is less permissive for neurite growth, quantitative comparisons were made of neurite lengths from neurons attached directly to crush sites and neurons attached to uncrushed regions. Since it is difficult to follow a single neurite from soma to growth cone in the case of high neuronal densities, the quantitative comparisons were derived from measurements of neurites from neurons that attached in lower densities. The mean length of neurites on crushed spinal cord white matter was signif-

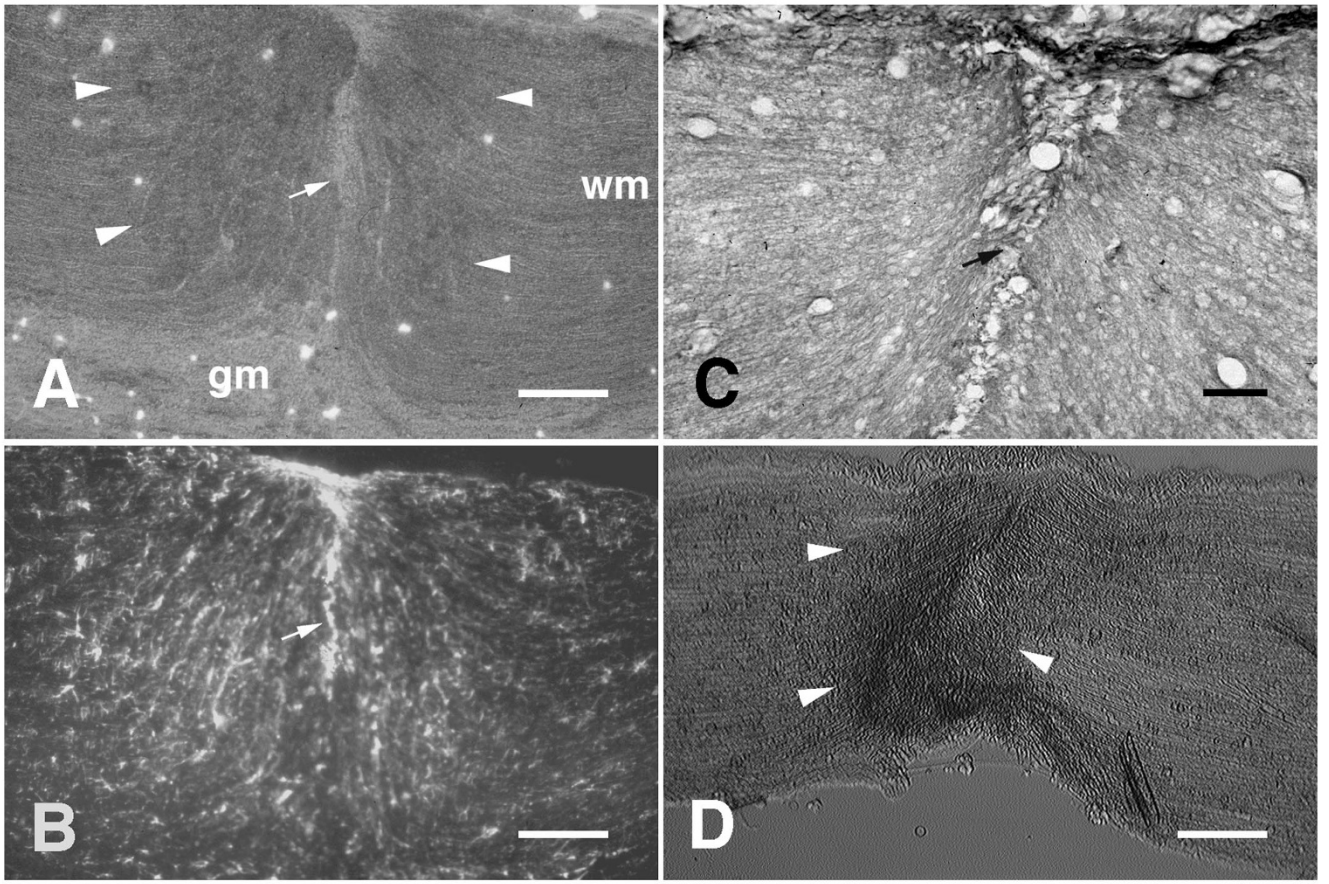

Figure 1
Ex vivo crush disrupts geometry. *A*, Phase-contrast photomicrograph of a horizontal cryostat section (the longitudinal axis is from left to right) containing spinal cord white matter (*wm*) that had been bilaterally crushed with forceps prior to freezing. The crushed white matter is evident from its increased optical density. The edges of the crushed segment of white matter are indicated by *white arrowheads*. A line of complete disruption can be seen near the middle of the crushed segment (*white arrow*). The optical density of crushed gray matter (*gm*) was not increased by the crush. *B*, GFAP immunoreactivity within the same field shown in panel *A*. Disruption of the normally parallel orientation of GFAP-labelled processes can be seen within the crush. *C*, An adjacent section of crushed spinal cord stained with Luxol-Fast Blue shows similar disruption to myelin. *D*, Phase-contrast photomicrograph of a longitudinal cryostat section of sciatic nerve that had been crushed with forceps prior to freezing. The crushed nerve tissue is evident from its increased optical density. The edges of the crushed segment of nerve are indicated by *white arrowheads*. Scale bars: *A*, *B*, 200 μm; *C*, 50 μm; *D*, 200 μm.

icantly reduced compared with that of neurites on uncrushed white matter (Fig. 3A; $p < 0.05$), indicating that regions of disrupted white matter geometry are inhibitory to neurite growth. To determine the effect of disrupted geometry on neurite orientation, quantitative comparisons were made of the orientations of these same neurites. The mean angular deviation of neurites from an orientation parallel to the longitudinal axis of the fiber tract on crush sites was significantly greater than that of neurites on uncrushed spinal cord white matter (Fig. 3B; $p < 0.001$). Moreover, the variance of this deviation on crushed white matter was significantly greater than that of neurites on uncrushed white matter [$F(30,37) = 3.788$; $p < 0.0001$]. This is consistent with the interpretation that neurites extend in a wider range of orientations on crushed white matter.

Neurite growth on sections of crushed sciatic nerve

The density of neurons and neurites was considerably greater on sections of sciatic nerve compared with that seen on spinal cord white matter. Similar to that on spinal cord white matter, neurite growth on uncrushed segments of sciatic nerve was extensive and oriented in parallel with the longitudinal axis of the nerve (Fig. 4A,E). However, as in the case of crushed spinal cord white matter, neurites rarely extended onto crushed sciatic nerve (Fig. 4A,C,E,G). As neurites approached the crushed tissue they often appeared to deviate from a par-

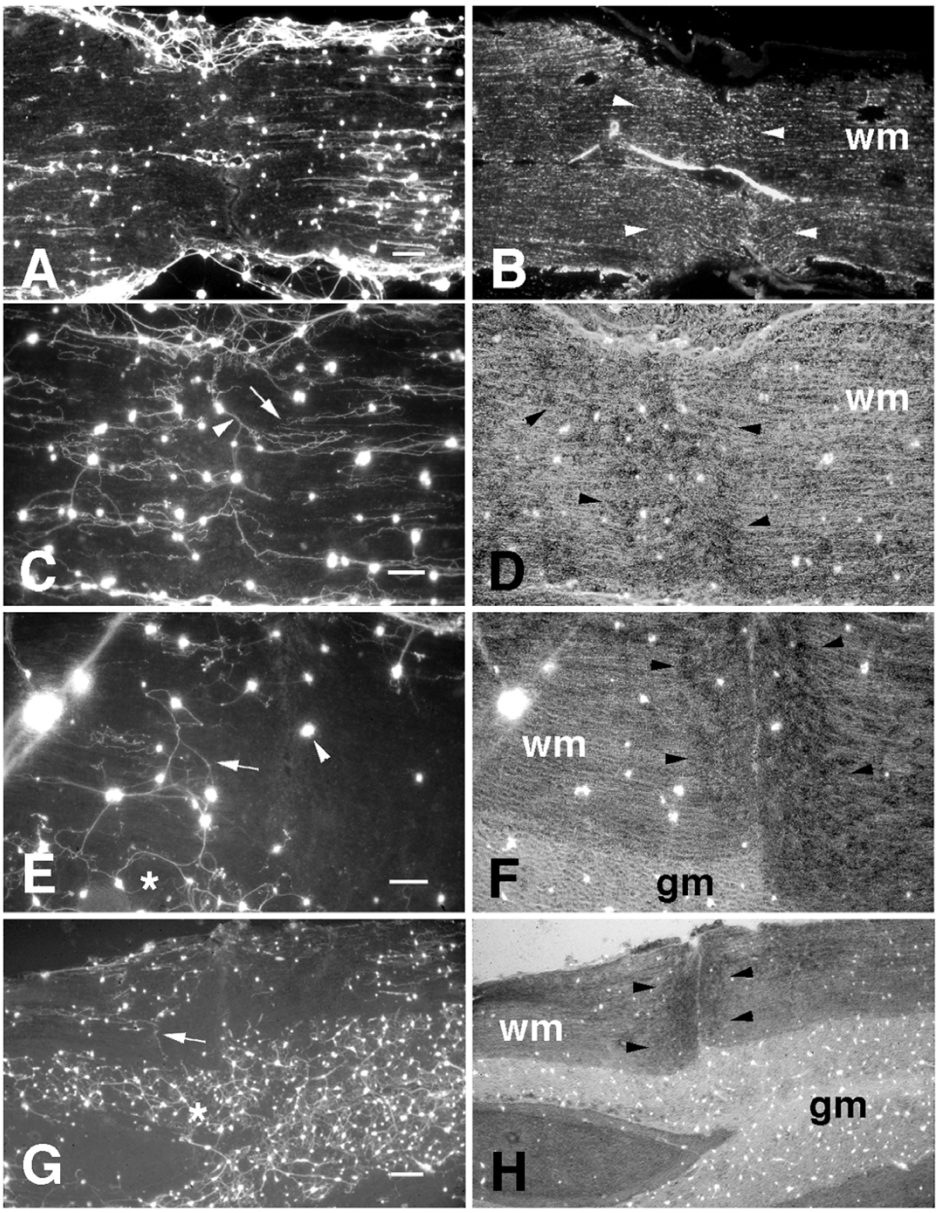

Figure 2
Neurite growth on ex vivo crushed spinal cord *A*, Fluorescein-labelled neurites extending on a horizontal section through crushed spinal cord white matter. Long parallel neurites extended on the uncrushed segments of white matter but did not extend onto crushed white matter. *B*, An adjacent section showing GFAP immunoreactivity within the crushed white matter (*wm*). Edges of the crush are indicated by *white arrowheads*. *C*, Neurites extending on crushed and uncrushed spinal cord white matter. Neurites extended in parallel on uncrushed segments of spinal cord white matter but terminated at edges of the crushed region of tissue (*white arrow*). Neurites extending from neurons attached directly on the crushed region often extended in non-parallel orientations and appeared to use each other as a substrate (*white arrowhead*). *D*, Phase-contrast photomicrograph of the same field shown in panel *C*. The crushed white matter is evident from its increased optical density. The edges of the crushed segment of white matter (*wm*) are indicated by *black arrowheads*. *E*, Neurites extending on crushed and uncrushed segments of spinal cord white matter. Several of these neurites appeared to use each other as a substrate as they approached the crushed tissue and turned in non-parallel orientations (*white arrow*). A neuron attached directly to crushed white matter did not extend a neurite (*white arrowhead*). Neurites extending on gray matter (*white asterisk*) appeared to be unaffected by the crush. *F*, Phase-contrast photomicrograph of the same field shown in panel *E*. *G*, Neurites extending on uncrushed white matter did not extend onto crushed white matter (*white arrow*). Neurites extending on gray matter (*white asterisk*) were not inhibited by crushed gray matter. *H*, Phase-contrast photomicrograph of the same field shown in panel *G*. *gm*, gray matter. Scale bars: *A*, 250 μm; *C*, *E*, 100 μm; *G*, 250 μm.

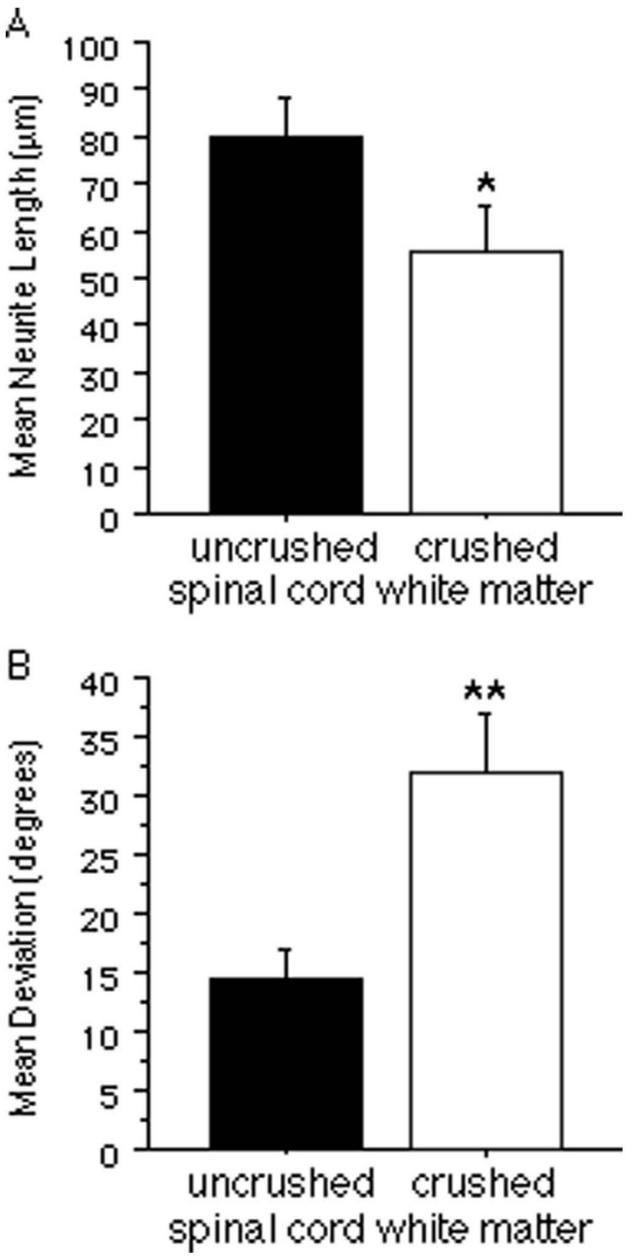

Figure 3
Comparisons of neurite growth on crushed and uncrushed spinal cord white matter. *A*, Neurite length on crushed segments of spinal cord white matter was significantly reduced compared with that on uncrushed segments. *B*, The angular deviation of neurites from an orientation parallelto the longitudinal axis of the underlying fiber tract was significantly greater on crushed segments of spinal cord white matter compared with that on uncrushed segments. All bars indicate mean + SEM (* $p < 0.05$; ** $p < 0.001$).

allel orientation and also appeared shorter in length (Fig. 4C,G).

Neurite density was quantified in relation to the crushed tissue by assessing the average total fluorescence at a range of spatial positions along the longitudinal axis and subtracting the fluorescence due to neuronal cell bodies. Differences in total plating density between culture experiments, culture dishes, and sections were normalized by dividing each value by the maximum fluorescence value within the same field. Using this quantification technique, a statistically significant reduction ($p < 0.0001$, comparing positions 100 μm on either side of crush edge) in neurite density was detected on crushed sciatic nerve tissue (Fig. 5A), suggesting that acutely crushed sciatic nerve tissue is inhibitory to neurite growth.

A similar quantification of neuronal density in relation to the crushed sciatic nerve showed that neuronal attachment was also significantly reduced ($p < 0.001$) on crushed sciatic nerve tissue (Fig. 5B). Since it is possible that the reduced neurite density on crushed sciatic nerve is a direct consequence of there being fewer neurons, a separate analysis was made comparing the lengths of neurites from neurons attached directly on crushed sciatic nerve with those attached on uncrushed sciatic nerve (Fig. 6A). Neurite length was significantly reduced on crushed sciatic nerve ($p < 0.0001$). To determine if the orientation of neurites is altered by crushed sciatic nerve tissue, the orientations of these neurites were also compared (Fig. 6B). The mean angular deviation of neurites from an orientation parallel to the longitudinal axis on crushed sciatic nerve was significantly greater than that of neurites on uncrushed sciatic nerve ($p < 0.0001$). Moreover, the variance of the deviation on crushed nerve was significantly greater than that on uncrushed nerve [$F(65,122) = 3.226$; $p < 0.0001$], indicating a wider range of orientations on crushed tissue.

Discussion

Central nervous system regeneration

Spinal cord injury disrupts the anatomical organization (geometry) of the cells and molecules that compose fiber tracts, including myelin, and elicits glial scarring, including astrogliosis and increased expression of CSPGs [30]. These latter factors inhibit neurite growth *in vitro* [19,20,21]. The success of axonal growth from neurons transplanted into white matter appears to depend on avoiding significant disruption of this geometry and the upregulation of CSPGs [17,18]. When avoided, extensive parallel axonal growth can occur. When disrupted, the pattern of CSPG expression is coincident with abortive axonal growth. These observations have supported the argument that CSPGs are the primary cause of axonal regeneration failure.

However, the relative contributions to abortive regeneration of CSPG upregulation and the disruption of the or-

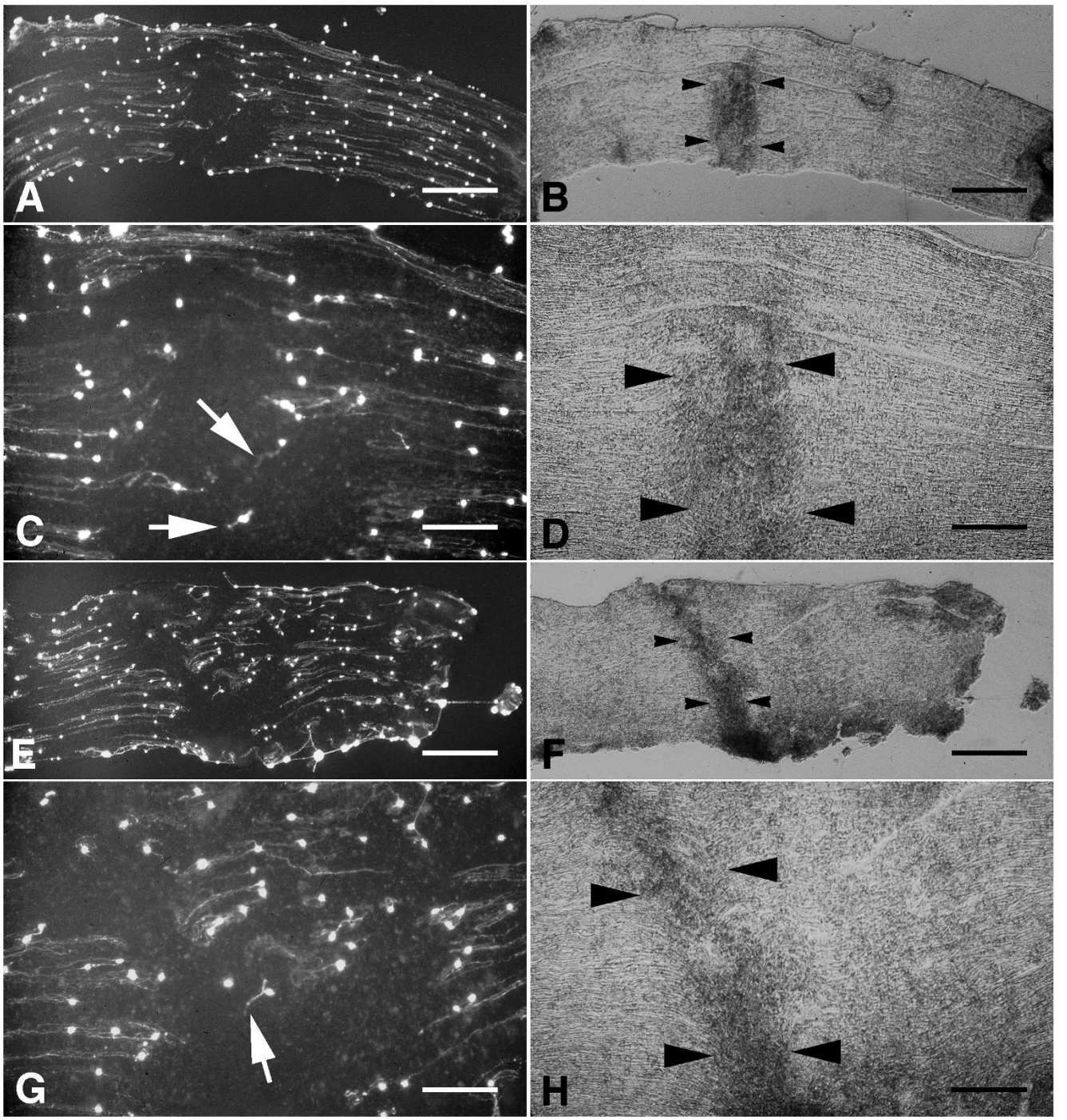

Figure 4
Neurite growth on ex vivo crushed sciatic nerve. *A*,*E*, Fluorescein-labelled neurites extending on longitudinal sections through crushed sciatic nerves. Long parallel neurites extended on uncrushed portions of the nerve sections but did not extend onto the crushed segments. Higher power photomicrographs of the crushed segments of the sections in panels *A* and *E* are shown in panels *C* and *G*, respectively. Neurites extending from neurons attached directly on crushed nerve tissue were usually shorter and oriented in non-parallel orientations (*white arrows*). *B*, *D*,*FH*,, Phase-contrast photomicrographs of the same fields shown in panels *AC*,,*EG*,, respectively. Crushed sciatic nerve is evident from its increased optical density. The edges of the crushed segments of sciatic nerve are indicated by *black arrowheads*. Scale bars: *A*, *B*, 500 μm; *C*, *D*, 200 μm; *E*, *F*, 500 μm; *G*, *H*, 200 μm.

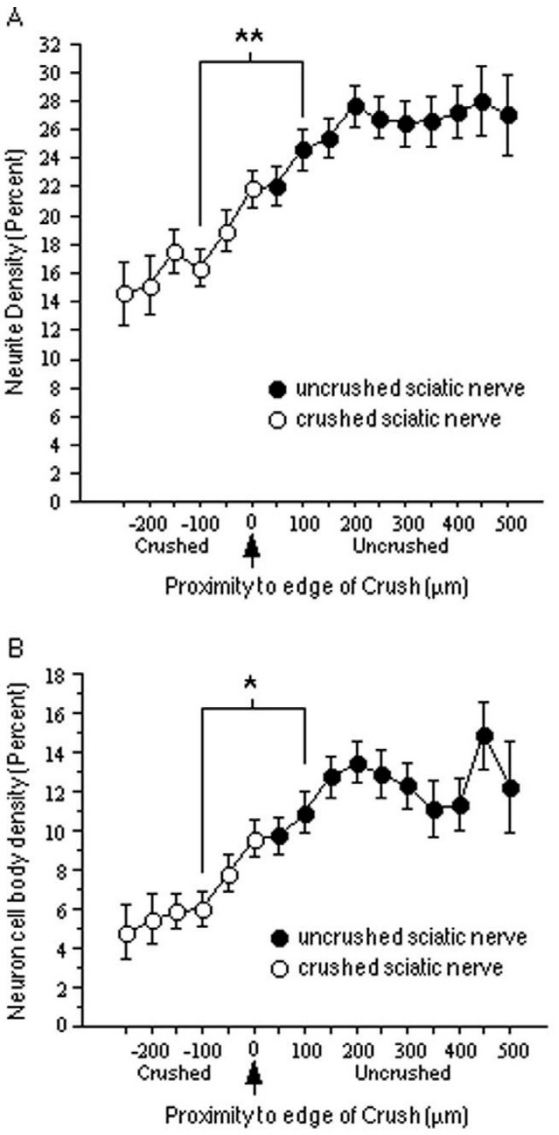

Figure 5
Neuron and neurite density on crushed sciatic nerve. *A*, Neurite density on sections of crushed sciatic nerve as a function of proximity to the crush (the *arrow* indicates the edge of the crushed tissue; distances < 0 indicate crushed nerve; distances > 0 indicate uncrushed nerve). The y-axis is the percentage of the maximum number of neurites found in the same field. The mean neurite density observed at longitudinal positions 100 μm into the crushed portions of the nerve tissue was significantly less than that on uncrushed nerve tissue 100 μm from the crush edge. *B*, Neuron density on sections of crushed sciatic nerve as a function of proximity to the crush. The y-axis is the percentage of the maximum number of neurons found in the same field. The mean neuron density observed at longitudinal positions 100 μm into the crushed portions of the nerve tissue was significantly less than that on uncrushed nerve tissue 100 μm from the crush edge. All bars indicate mean + SEM (** $p < 0.0001$; * $p < 0.001$).

ganization of cells and biochemical factors, such as, for example, myelin-associated inhibitors, that were present prior to injury (disrupted geometry) cannot be easily assessed *in vivo*. By the time axons initiate a growth response to the injury, the tissue has undergone considerable change, including CSPG upregulation. Disrupted tissue geometry may contribute to blocking axonal regeneration independently of glial scarring and CSPG upregulation.

Most previous attempts to establish an organotypic culture model of axonal growth on CNS white matter have failed because it was not possible to obtain attachment of neurons to white matter without enzymatically altering the substrate [31] or treating with neurotrophins [31,32] or conditioned medium [33]. It was recently shown that sympathetic neurons can attach to longitudinal sections of CNS white matter provided that they are grown under optimal conditions and plated in large numbers. Culture in Neurobasal medium [34] has been shown to optimize the survival of embryonic chick sympathetic neurons *in vitro* [35] and provides the necessary numbers. Consistent with the available data from both *in vivo* and *in vitro* studies, these neurons extend neurites in parallel on white matter and are inhibited from extending onto white matter from gray matter, indicating that these neurons are sensitive to the relevant inhibitory and growth-orienting cues found in white matter.

A limitation of tissue section culture is that it accounts for only two of the three dimensions normally present *in vivo*. However, the intent of this study was to examine the role of the parallel array of tissue elements in regulating axonal growth and the two-dimensional sections are longitudinal cuts through this three-dimensional parallel geometry. The behavior of growth cones on the sections cannot be assumed to be the same as that normally occurring in the more complex three-dimensional structure of the tissue in vivo. Nevertheless, the striking similarity to the parallel axonal growth within white matter observed from transplanted neurons *in vivo* [17,18,23,24,25,26,27,28,36] makes it unlikely that the pattern of neurite growth in tissue section culture is due to a limitation in the available degrees of freedom. In fact, the correspondence between the orientation of neurite growth in this assay and that observed *in vivo* suggests that tissue section culture models at least some of the relevant tissue properties and geometry. This same technique provides a unique opportunity to assess the response of neurites to injured tissue without glial scarring. Spinal cord was removed, bilaterally crushed, and immediately frozen to prevent additional injury-induced changes. Longitudinal sections were then used as substrata for neuronal cultures.

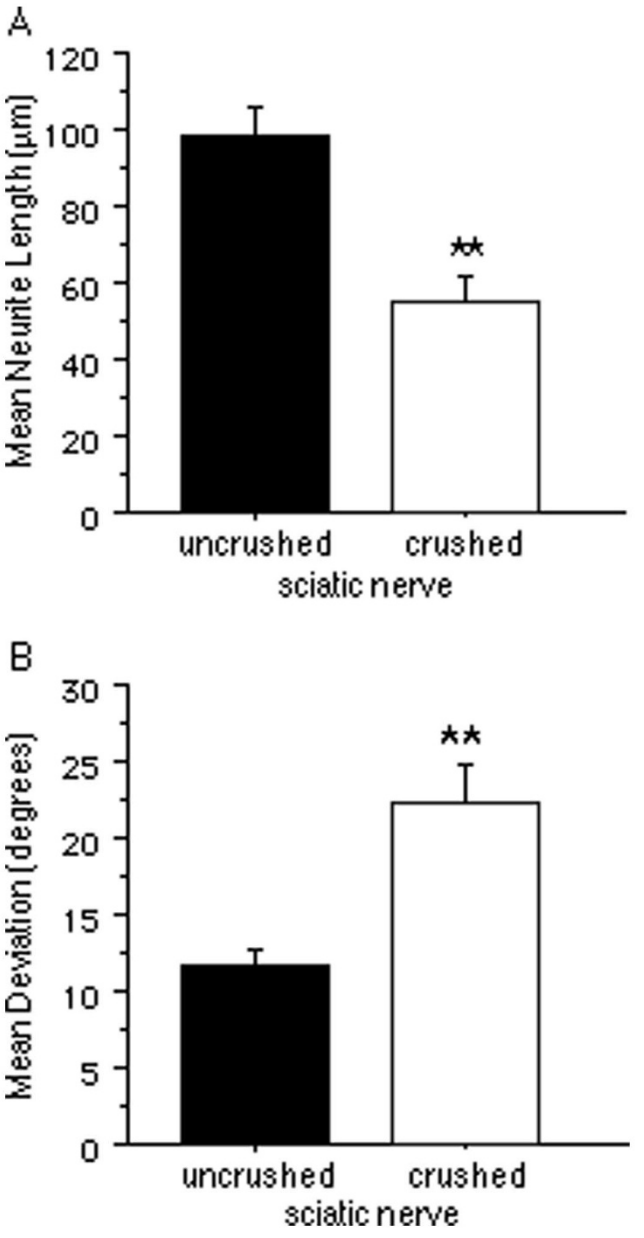

Figure 6
Comparisons of neurite growth on crushed and uncrushed sciatic nerve. *A*, The mean neurite length on crushed sciatic nerve was significantly less than that on uncrushed sciatic nerve. *B*, The mean angular deviation of neurites from an orientation parallel to the longitudinal axis of the underlying nerve was significantly greater on crushed nerve compared with that on uncrushed nerve. All bars indicate mean + SEM (** $p < 0.0001$).

It was evident from phase-contrast optics, GFAP immunoreactivity, and myelin staining that the crush manipulations disrupted the organization of spinal cord white matter. However, as assessed by GFAP immunohistochemistry, there was no indication of the dense astrogliotic matrix characteristic of glial scars [19,29]. Although patches of increased GFAP immunoreactivity appeared in the crushed tissue, these were likely due to increased accessibility and density of GFAP caused by crushing. The short period of time between crushing the tissue and freezing (less than 5 minutes) would have prevented astrogliosis. Moreover, CSPG immunohistochemistry showed no increase in CSPG expression.

On uncrushed white matter, neurites extended in parallel with the fiber tracts, as previously reported [22]. However, crushed white matter appeared to be relatively non-permissive for neurite growth. Like those on cross-sections of white matter [22], neurons attached directly on crushed white matter often extended non-parallel neurites or little neurite outgrowth at all. Moreover, neurites originating on uncrushed white matter were inhibited by crushed white matter. This is most like the situation *in vivo* when regenerating axons approach an injury site. These neurites often terminated abruptly as they approached crushed white matter, often turning in non-parallel directions and appeared to use each other as a substrate. A zone of complete tissue disruption was often present within the injury site but neurites rarely extended far enough onto the crushed tissue to encounter this zone.

Earlier studies using tissue section culture, in which virtually no neurons attached on white matter, concluded that white matter is nonpermissive for neurite growth [4,6,7,12,37,38]. This conclusion was premature in light of recent studies demonstrating that although white matter is less permissive for neuronal attachment than gray matter, it is highly permissive for neurite growth from those neurons that do attach, providing that this growth occurs in parallel with the fiber tract [22]. This parallel constraint on neurite growth may be mediated by myelin (Pettigrew and Crutcher, companion paper [http://www.biomedcentral.com/1471-2202/2/9]), and possibly, its neurite-growth inhibitory activity [5,8-16]. Because myelin is organized in parallel with the fiber tract, it may normally permit parallel neurite growth while inhibiting non-parallel growth.

This same inhibitory activity might also contribute to the non-permissive properties of crushed white matter. An injury to a myelinated tract may disrupt the parallel organization of myelin, thereby contributing to a relatively non-permissive environment for axonal regeneration. Consistent with this hypothesis, neurites were unimpeded by crushed gray matter, exhibiting essentially random growth as seen on uncrushed gray matter. Injury may also unmask inhibitors that are normally inaccessible to growing axons. One inhibitor, myelin-associated glycoprotein (MAG), is reportedly expressed within, but not

on outer surfaces of, myelin sheaths [8]. An injury to white matter could presumably expose these factors by disrupting the sheaths. As a result, axons approaching injured white matter would encounter disorganized myelin debris containing inhibitors. In combination with disruption of the permissive substrates upon which axons normally grow, disrupted white matter could become a non-permissive environment due to exposure of inhibitors. Although factors other than myelin-associated inhibitors likely play a role in preventing axonal regeneration [3], these data suggest that disrupted geometry may contribute to the non-permissive properties of the injured tissue.

Peripheral nervous system regeneration

Neurites also extended on uncrushed segments of sciatic nerve. In fact, consistent with previous reports [4,12], neuronal attachment and neurite density were greater on sciatic nerve sections than on CNS white matter. The parallel orientation of neurite growth on peripheral nerve has been reported [39,40,41] but little mention has been made of this phenomenon. Such growth might be due to non-permissive factors aligned in parallel with the nerve that constrain neurites to this orientation. In fact, neurite inhibitors, such as MAG [8] and CSPGs [42], are normally distributed in parallel within nerves. It is possible that disrupting the geometry of these inhibitors creates an obstacle to growing neurites. On the other hand, strong neurite-promoters such as laminin, are also present in peripheral nerves. In fact, laminin has been shown to over-ride the inhibition of neurite growth caused by MAG [43]. Therefore, it is possible that the combination of inhibitory and stimulatory factors ultimately determines the permissiveness of the substrate. One of the limitations of the in vitro approach used here is that alterations in the proportion of such factors might not reflect the actual conditions obtained in vivo. Other changes in the tissue, such as haptotactic changes or lipid blebbing could conceivably contribute to the non-permissive substrate properties obtained after crush injury and tissue section culture.

Whatever changes are ultimately responsible, neurites extending on uncrushed portions of sciatic nerve, like those on spinal cord white matter, abruptly terminated upon reaching crushed portions of the tissue. Moreover, both neuronal attachment and neurite density on crushed sciatic nerve were significantly reduced compared with uncrushed nerve. The reduced neurite density cannot be attributed solely to reduced neuronal attachment. Direct comparisons of neurite growth on crushed and uncrushed sciatic nerve were made independently of differences in neuronal density. Consistent with the hypothesis that crushed sciatic nerve is less permissive for neurite growth, neurites were significantly shorter on crushed sciatic nerve than on uncrushed sciatic nerve. Neurites extending on crushed nerve were also significantly less parallel.

That crushed sciatic nerve is relatively non-permissive to growing neurites may seem surprising since axonal regeneration normally occurs in peripheral nerves. However, regenerating axons do not encounter regions of acute injury in vivo. During the lag between injury and robust growth, extensive changes occur within the injury site, including clearance of degeneration debris. In fact, these data are consistent with studies of mutant Ola mice in which Wallerian degeneration is delayed and peripheral nerve regeneration is impaired [44,45]. Axonal regeneration, although normally successful in peripheral nerves, may be nevertheless dependent on degeneration of the distal nerve segment and subsequent reconstruction of the normal tissue geometry.

Conclusions

These results support a surprising hypothesis. Both white matter and peripheral nerves may contain inhibitory factors whose normal role is to constrain axons to a parallel orientation by preventing collateral sprouting. In both situations, disruption of tissue geometry would result in a substrate that is less navigable by growing axons. However, whereas in peripheral nerves the appropriate geometry is reconstructed, in white matter, such reconstruction apparently fails or does not succeed in sufficient time to permit regeneration. In addition, glial scarring has long been suspected to contribute to the non-permissive environment encountered by regenerating axons in the CNS.

What may then distinguish white matter and peripheral nerves with regard to regenerative potential is the rate of degeneration and/or reconstruction of the peritraumatic region and distal stump. Wallerian degeneration normally occurs much faster in peripheral nerves than in white matter [46,47,48]. Although myelin clearance within the peritraumatic region of central fiber tracts begins soon after injury, this clearance proceeds slowly. Myelin debris have been reported within peritraumatic regions of white matter as late as 52 to 60 days following injury [48,49]. Even if myelin debris are ultimately cleared from the peritraumatic region, this may not be sufficient to permit axonal regeneration. Although neurons appear to possess the intrinsic capacity to regenerate their axons, this capacity may not be retained indefinitely following injury. In the mutant Ola mouse, Wallerian degeneration is significantly delayed following injury to peripheral nerves but nevertheless occurs. However, nerve regeneration in these mutants never reaches the capacity observed in injured nerves of wild-type mice [44]. If a similar time-constraint exists in

white matter then degeneration of the distal stump must occur sufficiently within a critical time period to allow regeneration. The slow rate of Wallerian degeneration and reduced restoration of white matter geometry following injury, compared with that in peripheral nerves, may be a key reason why axonal regeneration in the CNS is impaired.

Materials and Methods

Preparation of substrata

Sprague-Dawley Rats (maintained in the University of Cincinnati vivarium in accordance with the NIH guide for the care of research animals) were deeply anesthetized using 4 ml/kg i.p. of pentobarbital sodium solution (50 mg/ml; Abbott Laboratories, North Chicago, IL) and decapitated. The spinal cords and sciatic nerves were rapidly removed and crushed bilaterally using forceps and immediately frozen at -80°C. Sixteen micron thick horizontal sections of spinal cord or sciatic nerve through the crush injury were subsequently prepared using a cryostat and thaw-mounted onto uncoated 35 mm plastic culture dishes (Fisher Scientific, Cincinnati, OH). Substrata were kept at -20°C until plating 2 hours later.

Tissue culture

Lumbar sympathetic chain ganglia were dissected from embryonic day 10 Leghorn chicken embryos (Spafas, Inc., Boston, MA) in Ham's F12 medium (Sigma, St. Louis, MO). The chain ganglia were incubated with 0.25% trypsin (Sigma) for 20 minutes at 37°C. Trypsinization was subsequently blocked by exposure to 100% heat-inactivated fetal bovine serum (Harlan Bioproducts for Science, Indianapolis, IN) for 5 minutes and washed 2 times with Ham's F12 medium. The tissue was then dissociated by gentle trituration using flamed Pasteur pipets (Fisher; Cat. No. 13-678-6A) and the cell suspension was seeded onto the prepared tissue sections. All cultures were grown in serum-free Neurobasal medium (2 ml per dish) supplemented with B27 (Gibco BRL, Grand Island, NY; 50:1 v/v), 0.5 mM L-glutamine (Sigma) and 100 units/ml penicillin-streptomycin (Gibco; Cat. No. 15140-015) in a humidified environment at 37°C and 5.5 to 6.0% CO_2.

Evaluation of neurite growth

After 7 days in culture, all media were removed and replaced with Ham's F12 medium. Neurons and neurite growth were labelled by incubating each dish with 2.5 ng/ml of 5-carboxyfluorescein diacetate, acetoxymethyl ester (vital dye; Molecular Probes, Eugene, OR) for 45 to 90 minutes at 37°C. Subsequently, all media were removed and replaced with fresh Ham's F12 medium. The cultures were then visualized using a Nikon Diaphot fluorescent microscope with a fluorescein filter and a 4x or 10x objective. Substrate histology was visualized using phase-contrast optics. Photomicrographs were captured with a Nikon 35 mm camera. In other cases, digital images were captured to a Power Macintosh microcomputer with a Data Translation framegrabber card and electronically enhanced to increase contrast.

Quantification of the spatial distribution (density) of neurons and neurites

The relative distribution of neurons and neurites over a longitudinal distance spanning the crushed and uncrushed portions in sciatic nerve sections was assessed using a customized macro program written for NIH Image 1.60 software. The orientations of the longitudinal axes and the spatial extent of the crushed portions of the sciatic nerve sections used as substrata were assessed using phase-contrast digital images showing the anatomy of the section but not the neurons and neurites within the field. Each field consisted of the adjacent uncrushed segments of nerve on either side of a crushed segment, which could be identified by its greater optical density (e.g., Fig. 4B,F). The orientation of the fiber tract was measured by drawing a line parallel to its edges and measuring the angle of this line using NIH Image 1.60 software. A rectangular contour was then drawn selecting the uncrushed segment of the nerve section to the left of the crushed segment using the NIH Image rectangle tool. This contour was drawn to fit within the limits of the tissue section while selecting a maximum area of the section to the left of the crush. The right edge of the rectangle was drawn to coincide with the left edge of the crush. The procedure was then repeated for the uncrushed segment of nerve section to the right of the crush (in this case the left edge of the drawn rectangle coincided with the right edge of the crush). The traced longitudinal axis as well as both rectangular regions drawn over the uncrushed segments were recorded by the macro program.

A fluorescence image of the same field showing only neurons and neurites labelled with vital dye was then opened and automatically rotated using a macro function so that the longitudinal axis of the nerve was horizontal. The image was then thresholded to optimize the signal (the neurites and neurons)-to-noise ratio. A macro function then automatically measured the average gray value at each position along the longitudinal axis of the nerve including the crush. This value is proportional to the number of fluorescently-labelled neurons and neurites at each position. The procedure was then repeated after adjusting the threshold so that only the neuronal cell bodies were shown.

The following data were then computed automatically by the macro. The average gray values for both total fluorescence (cell bodies + neurites) and cell bodies only were computed for each 10 pixel-wide bin along the longitudi-

nal axis. The macro automatically assessed the position of the crush given the rectangular boxes drawn by the observer and one-dimensional longitudinal coordinates for each of the bins were assigned. Each edge of the crush was defined as an origin (x = 0). Spatial locations within the crush were defined using negative-valued coordinates and spatial locations on uncrushed segments were defined using positive-valued coordinates. The magnitude of the coordinates defined the distance, in pixels, into the crush or away from the crush, respectively. The macro also reported the maximum average gray value over all positions within each field for both the total fluorescence (cell bodies + neurites) and cell bodies without neurites.

The final data were generated using Statview 5.0 (Abacus Concepts). A measure of neurites, excluding cell bodies, was computed for each bin by subtracting the cell bodies-only values from the total fluorescence values. The final measures of neurite and neuron density were normalized by dividing by their respective maximums in each field providing, for each bin, a percentage of the maximum number of neurites or neurons found in the field. For example, if in a given optical field on a given tissue section, the maximum fluorescence value was found to be at a position 400 μm distal to the border of the crushed tissue then all fluorescence values measured within this field were divided by the fluorescence value measured at the 400 μm position. This was intended to control for variability in plating density from culture to culture and section to section. The spatial coordinates for each bin were converted to micrometers using a standard. All statistical comparisons were made using one-tailed, unpaired Student's t-tests.

Quantification of neurite length and orientation

The orientations of the longitudinal axes and the spatial extent of the crushed regions were assessed using phase contrast optics. The orientation of the fiber tract was measured by drawing a line parallel to its edges and measuring the angle of this line using NIH Image 1.60 software. A contour was then traced around the perimeter of the crushed region, as assessed by its increased optical density, using the polygon tool provided by NIH Image. Both the orientation of the longitudinal axis and the spatial extent of the crush were recorded by a customized NIH Image macro.

This image was then closed and replaced by an image of the same field showing the neurons and their neurites but not the anatomy of the section. Neurite length and orientation were then assessed. A neuron was included for analysis if its neurite did not form fascicles with other neurites and if it was possible to visually follow the entire length of the neurite. Neurite length was assessed by tracing the neurite using the straight-line tool in NIH Image. The net length, i.e. the straight-line distance between the cell body and growth cone, was measured in pixels and then converted to micrometers using a known standard. From vector arithmetic we know that this distance is the weighted (by segment length) average of the orientations of each of the segments along the total length of the neurite. The macro program automatically determined whether the neuronal cell body was located within the polygon-delimited spatial extent of the crush and classified each neuron as being attached to either the crushed portion of the section or an uncrushed portion. Neurite orientation was recorded by the macro by measuring the angle of the line traced over the neurite.The final measure of orientation for each neurite, the deviation from an orientation parallel to the longitudinal axis of the tract, is the acute angle between the neurite and the longitudinal axis of the tract without regard to the polarity of either. This value ranged from 0° to 90° where 0° indicated a neurite growing in parallel with the longitudinal axis of the underlying tract and 90° indicated a neurite oriented perpendicular to the tract. All statistical comparisons were made using one-tailed, unpaired Student's t-tests.

GFAP immunohistochemistry

Glial Fibrillary Acidic Protein (GFAP) was labelled in the same spinal cord sections on which neurons had been cultured. The sections were incubated with a Cy3-conjugated monoclonal antibody raised against porcine GFAP (Sigma; Product No. C9205) diluted in Ham's F12 medium (1:400) for 90 minutes at 37°C. The medium in each dish was then removed and replaced with 1.5 ml of fresh Ham's F12 medium. The sections were then visualized using a Nikon Diaphot fluorescent microscope with a rhodamine filter and a 4x or 10x objective. Photomicrographs were captured with a Nikon 35 mm camera.

CSPG immunohistochemistry

Chondroitin sulfate proteoglycan (CSPG) staining was carried out in adjacent spinal cord sections using the monoclonal antibody CS-56 raised against chicken chondroitin sulfate. Sixteen micron thick sections were mounted on gelatin-coated slides and postfixed in 4% paraformaldehyde for 12 minutes at room temperature and then rinsed 4 times with .1 M PBS. The sections were incubated in NGS blocking buffer [4% normal goat serum (NGS; Vector Laboratories, Burlingame, CA; Cat. No. S-1000) + .2% Triton-X (Sigma) in .1 M PBS] for 1 hour at room temperature and rinsed 4 times with .1 M PBS + .2% Triton-X. The sections were then incubated with the CS-56 antibody (Sigma; Product No. C8035; 1:25 in NGS blocking buffer) overnight at 4°C. Subsequently, the sections were rinsed 4 times with .1 M PBS + .2% Triton-X and incubated for 1 hour at room tempera-

ture with the secondary antibody (FITC-conjugated sheep anti-mouse IgG; Boehringer-Mannheim, Indianapolis, IN; Cat. No. 821-462; 1:200 in 4% NGS). The sections were rinsed once with .1 M PBS + .2% Triton-X, 3 times with .1 M PBS and then coverslipped using 95% glycerol as a mounting solution. The sections were then visualized using a Nikon Microphot fluorescent microscope with a fluorescein filter and a 4x, 10x, 20x or 40x objective. Photomicrographs were captured with a Nikon 35 mm camera. Reliability of CSPG immunohistochemistry was verified by positive staining of dorsal root entry zones in transverse sections of unfixed spinal cord.

Myelin histochemistry

Adjacent sections were stained using the Luxol Fast Blue technique for visualizing myelin [50]. Sixteen micron thick sections were mounted on gelatin-coated slides and post-fixed in 4% paraformaldehyde for 30 minutes at room temperature. The sections were then dehydrated by immersion in 70% ethanol (3 immersions, 6 minutes each) and then transferred to 95% ethanol for 6 minutes. The sections were then stained with Luxol Fast Blue (in 95% ethanol) for 13 minutes at room temperature, rinsed twice with 100% ethanol and cleared overnight in a third 100% ethanol rinse. Subsequently, the sections were rinsed 3 times in xylene and coverslipped using Permount (Fisher) as a mounting solution. The sections were visualized using a Nikon Microphot fluorescent microscope and a 10x objective. Photomicrographs were captured with a Nikon 35 mm camera.

Acknowledgments

This work was supported by the Mayfield Education and Research Foundation. A portion of this work has been reported in abstract form at the Eighth International Symposium on Neural Regeneration and at the 2000 meeting of the Society for Neuroscience.

References

1. Ramón y Cajal S: *Degeneration and Regeneration of the Nervous System. London, U.K.: Oxford University Press;* 1928
2. David S, Aguayo AJ: **Axonal elongation into peripheral nervous system "bridges" after central nervous system injury in adult rats.** *Science* 1981, **214**:931-933
3. Berry M, Hall S, Rees L, Carlile J, Wyse JP: **Regeneration of axons in the optic nerve of the adult Browman-Wyse (BW) mutant rat.** *J Neurocytol* 1992, **21**:426-448
4. Carbonetto S, Evans D, Cochard P: **Nerve fiber growth in culture on tissue substrata from central and peripheral nervous systems.** *J Neurosci* 1987, **7**:610-620
5. Caroni P, Schwab ME: **Two membrane protein fractions from rat central myelin with inhibitory properties for neurite growth and fibroblast spreading.** *J Cell Biol* 1988, **106**:1281-1288
6. Crutcher KA: **Tissue sections from the mature rat brain and spinal cord as substrates for neurite outgrowth in vitro: extensive growth on gray matter but little growth on white matter.** *Exp Neurol* 1989, **104**:39-54
7. Crutcher KA, Privitera M: **Axonal regeneration on mature human brain tissue sections in culture.** *Ann Neurol* 1989, **26**:580-583
8. Filbin MT: **Myelin-associated glycoprotein: a role in myelination and in the inhibition of axonal regeneration?** *Curr Opin Neurobiol* 1995, **5**:588-595
9. McKerracher L, David S, Jackson DL, Kottis V, Dunn RJ, Braun PE: **Identification of myelin-associated glycoprotein as a major myelin-derived inhibitor of neurite growth.** *Neuron* 1994, **13**:805-811
10. Mukhopadhyay G, Doherty P, Walsh FS, Crocker PR, Filbin MT: **A novel role for myelin-associated glycoprotein as an inhibitor of axonal regeneration.** *Neuron* 1994, **13**:757-767
11. Niederöst BP, Zimmermann DR, Schwab ME, Bandtlow CE: **Bovine CNS myelin contains neurite growth-inhibitory activity associated with chondroitin sulfate proteoglycans.** *J Neurosci* 1999, **19**:8979-8989
12. Savio T, Schwab ME: **Rat CNS white matter, but not gray matter, is nonpermissive for neuronal cell adhesion and fiber outgrowth.** *J Neurosci* 1989, **9**:1126-1133
13. Schwab ME, Caroni P: **Oligodendrocytes and CNS myelin are nonpermissive substrates for neurite growth and fibroblast spreading in vitro.** *J Neurosci* 1988, **8**:2381-2393
14. Schwab ME, Schnell L: **Channeling of developing rat corticospinal tract axons by myelin-associated neurite growth inhibitors.** *J Neurosci* 1991, **11**:709-721
15. Schwab ME, Thoenen H: **Dissociated neurons regenerate into sciatic but not optic nerve explants in culture irrespective of neurotrophic factors.** *J Neurosci* 1985, **5**:2415-2423
16. Schwab ME, Bandtlow CE, Nicholls J: **Developmental expression of myelin-associated neurite growth inhibitors correlates with the loss of regeneration after spinal cord lesions in the opposum.** *Soc Neurosci Abstr* 1993, **19**:283-219
17. Davies SJ, Fitch MT, Memberg SP, Hall AK, Raisman G, Silver J: **Regeneration of adult axons in white matter tracts of the central nervous system.** *Nature* 1997, **390**:680-683
18. Davies SJ, Goucher DR, Doller C, Silver J: **Robust regeneration of adult sensory axons in degenerating white matter of the adult rat spinal cord.** *J Neurosci* 1999, **19**:5810-5822
19. McKeon RJ, Schreiber RC, Rudge JS, Silver J: **Reduction of neurite outgrowth in a model of glial scarring following CNS injury is correlated with the expression of inhibitory molecules on reactive astrocytes.** *J Neurosci* 1991, **11**:3398-3411
20. McKeon RJ, Höke A, Silver J: **Injury-induced proteoglycans inhibit the potential for laminin-mediated axon growth on astrocytic scars.** *Exp Neurol* 1995, **136**:32-43
21. Snow DM, Lemmon V, Carrino DA, Caplan AI, Silver J: **Sulfated proteoglycans in astroglial barriers inhibit neurite outgrowth in vitro.** *Exp Neurol* 1990, **109**:111-130
22. Pettigrew DB, Crutcher KA: **White matter of the CNS supports or inhibits neurite outgrowth in vitro depending on geometry.** *J Neurosci* 1999, **19**:8358-8366
23. Davies SJ, Field PM, Raisman G: **Long fibre growth by axons of embryonic mouse hippocampal neurons microtransplanted into the adult rat fimbria.** *Eur J Neurosci* 1993, **5**:95-106
24. Davies SJ, Field PM, Raisman G: **Long interfascicular axon growth from embryonic neurons transplanted into adult myelinated tracts.** *J Neurosci* 1994, **14**:1596-1612
25. Humpel C, Bygdeman M, Olson L, Strömberg I: **Human fetal neocortical tissue grafted to rat brain cavities survives, leads to reciprocal nerve fiber growth, and accumulates host IgG.** *J Comp Neurol* 1994, **340**:337-348
26. Lehman MN, Lesauter J, Silver R: **Fiber outgrowth from anterior hypothalamic and cortical xenografts in the third ventricle.** *J Comp Neurol* 1998, **391**:133-145
27. Wictorin K, Brundin P, Gustavii B, Lindvall O, Björklund A: **Reformation of long axon pathways in adult rat central nervous system by human forebrain neuroblasts.** *Nature* 1990, **347**:556-558
28. Wictorin K, Brundin P, Sauer H, Lindvall O, Björklund A: **Long distance directed axonal growth from human dopaminergic mesencephalic neuroblasts implanted along the nigrostriatal pathway in 6-hydroxydopamine lesioned adult rats.** *J Comp Neurol* 1992, **323**:475-494
29. Fitch MT, Doller C, Combs CK, Landreth GE, Silver J: **Cellular and molecular mechanisms of glial scarring and progressive cavitation: in vivo and in vitro analysis of inflammation-induced secondary injury after CNS trauma.** *J Neurosci* 1999, **19**:8182-8198
30. Lemons ML, Howland DR, Anderson DK: **Chondroitin sulfate proteoglycan immunoreactivity increases following spinal cord injury and transplantation.** *Exp Neurol* 1999, **160**:51-65
31. Zuo J, Neubauer D, Dyess K, Ferguson TA, Muir D: **Degradation of chondroitin sulfate proteoglycan enhances the neurite-pro-**

moting potential of spinal cord tissue. *Exp Neurol* 1998, **154**:654-662
32. Chui SW, Yip HK, So K-F: **Neurite outgrowth of embryonic DRG neurons on optic nerve sections are promoted by neurotrophic factors.** *Soc Neurosci Abstr* 1998, **24**:20-24
33. Carpenter MK, Hassinger TD, Whalen LR, Kater SB: **CNS white matter can be altered to support neuronal outgrowth.** *J Neurosci Res* 1994, **37**:1-14
34. Brewer GJ, Torricelli JR, Evege EK, Price PJ: **Optimized survival of hippocampal neurons in B27-supplemented Neurobasal, a new serum-free medium combination.** *J Neurosci Res* 1993, **35**:567-576
35. Pettigrew DB, Crutcher KA: **Neurobasal medium promotes greater survival of embryonic chick sympathetic neurons than Ham's F12 medium.** *Soc Neurosci Abstr* 1996, **22**:299-215
36. Wictorin K, Lagenaur CF, Lund RD, Björklund A: **Efferent projections to the host brain from intrastriatal mouse-to-rat grafts: time course and tissue-type specificity as revealed by a mouse specific neuronal marker.** *Eur J Neurosci* 1991, **3**:86-101
37. Watanabe E, Murakami F: **Preferential adhesion of chick central neurons to the gray matter of the central nervous system.** *Neurosci Lett* 1989, **97**:69-74
38. Watanabe E, Murakami F: **Cell attachment to and neurite outgrowth on tissue sections of developing, mature and lesioned brain: the role of inhibitory factor(s) in the CNS white matter.** *Neurosci Res (N Y)* 1990, **8**:83-99
39. Anand U, McMahon SB, Cohen J: **Preferential growth of neonatal rat dorsal root ganglion cells on homotypic peripheral nerve substrates in vitro.** *Eur J Neurosci* 1996, **8**:649-657
40. Sandrock AW Jr, Matthew WD: **Identification of a peripheral nerve neurite growth-promoting activity by development and use of an in vitro bioassay.** *Proc Natl Acad Sci U S A* 1987, **84**:6934-6938
41. Shewan D, Berry M, Bedi K, Cohen J: **Embryonic optic nerve tissue fails to support neurite outgrowth by central and peripheral neurons in vitro.** *Eur J Neurosci* 1993, **5**:809-817
42. Zuo J, Hernandez YJ, Muir D: **Chondroitin sulfate proteoglycan with neurite-inhibiting activity is up-regulated following peripheral nerve injury.** *J Neurobiol* 1998, **34**:41-54
43. David S, Braun PE, Jackson DL, Kottis V, McKerracher L: **Laminin overrides the inhibitory effects of peripheral nervous system and central nervous system myelin-derived inhibitors of neurite growth.** *J Neurosci Res* 1995, **42**:594-602
44. Perry VH, Brown MC: **Role of macrophages in peripheral nerve degeneration and repair.** *Bioessays* 1992, **14**:401-406
45. Brown MC, Lunn ER, Perry VH: **Consequences of slow Wallerian degeneration for regenerating motor and sensory axons.** *J Neurobiol* 1992, **23**:521-536
46. Bignami A, Ralston HJd: **The cellular reaction to Wallerian degeneration in the central nervous system of the cat.** *Brain Res* 1969, **13**:444-461
47. Daniel PM, Strich SJ: **Histological observations on Wallerian degeneration in the spinal cord of the baboon, Papio papio.** *Acta Neuropathol (Berl)* 1969, **12**:314-328
48. Lampert PW, Cressman MR: **Fine-structural changes of myelin sheaths after axonal degeneration in the spinal cord of rats.** *Am J Pathol* 1966, **49**:1139-1155
49. Wakefield CL, Eidelberg E: **Electron microscopic observations of the delayed effects of spinal cord compression.** *Exp Neurol* 1975, **48**:637-646
50. Humason GL: *Animal Tissue Techniques. San Francisco, CA.: W. H. Freeman and Company;* 1972